Ruthenium Oxyl Radical Complex Containing *o*-Quinone Ligand Detected by ESR Measurements of Spin Trapping Technique

Katsuaki Kobayashi, Hideki Ohtsu, Tohru Wada, and Koji Tanaka
Institute for Molecular Science, CREST, Japan Science and Technology Corporation and Department of Structural Molecular Science, Graduate University for Advanced Studies, 38 Nishigonaka, Myodaiji, Okazaki, Aichi 444-8585

(Received May 23, 2002; CL-020450)

Ruthenium-quinone complex containing an aqua ligand, $[Ru^{II}(trpy)(35tBu_2Q)(OH_2)](ClO_4)_2$ (trpy=2,2′:6′,2″-terpyridine, $35tBu_2Q$=3,5-di-*tert*-butyl-1,2-benzoquinone) underwent deprotonation of an aqua ligand accompanied with intramolecular electron transfer from O^{2-} ligand to quinone ligand generating $O^{\bullet-}$ ligand.

Much attention has been paid to transition metal complexes containing quinone ligands in the areas of inorganic, organic, and biological chemistries.[1–5] Quinone (Q) is an electrochemically active ligand and undergoes stepwise reduction to yield semiquinone (SQ) and catecholate (Cat). The noticeable feature of metal-quinone complexes, therefore, is charge distribution between metal ion and the quinone ligand on account of accessible reduction states of the quinone ligand.[1–5] Pierpont et al. have synthesized a variety of ruthenium-quinone complexes,[4,5] which substantially serve the understanding of the structure and physicochemical properties of the complexes. Meyer et al. have demonstrated that oxidation of Ru^{II}-aqua complexes is accompanied with deprotonation of the aqua protons to form Ru^{IV}-oxo species.[6] On the contrary, dissociation of the aqua protons of aqua-ruthenium-quinone complexes is expected to give pronounced influences on charge distribution of the ruthenium-quinone moiety.

We have recently reported a ruthenium-quinone complex containing an aqua ligand, $[Ru^{II}(trpy)(35tBu_2Q)(OH_2)](ClO_4)_2$ (trpy=2,2′:6′,2″-terpyridine, $35tBu_2Q$=3,5-di-*tert*-butyl-1,2-benzoquinone) (**1**, $[Ru^{II}Q(OH_2)](ClO_4)_2$).[7] This communication describes the detailed physicochemical properties of **1** in the presence of various amounts of a base and the detection of ruthenium-semiquinone oxyl radical complex, which is generated in the deprotonation of the aqua ligand, by means of the spin trapping technique.

UV-vis spectrum of **1** in a CH_2Cl_2 solution shows the characteristic electronic absorption band at 600 nm ($\varepsilon = 16800\,M^{-1}\,cm^{-1}$) due to the charge-transfer transition of Ru^{II} to quinone (MLCT).[4,5,7,8] An addition of less than 1 equiv of a base such as *t*BuOK to the solution results in blue shift of the intense band at 600 nm to 576 nm ($\varepsilon = 16700\,M^{-1}\,cm^{-1}$) as shown in Figure 1. Such a blue shift caused by the addition of 1 equiv of *t*BuOK is consistent with the blue-shifted absorption band of $[Ru^{II}(trpy)(35tBu_2Q)(AcO^-)]^+$ (586 nm, $\varepsilon = 17000\,M^{-1}\,cm^{-1}$),[8] with an anionic ligand (AcO^-) as compared with that of $[Ru^{II}(trpy)(35tBu_2Q)(OH_2)]^{2+}$ (600 nm, $\varepsilon = 16800\,M^{-1}\,cm^{-1}$). Thus, the characteristic absorption band at 576 nm can be assigned to the MLCT band of $[Ru^{II}(trpy)(35tBu_2Q)(OH^-)]^+$ ($[Ru^{II}Q(OH^-)]^+$) which is the deprotonation form of $[Ru^{II}Q(OH_2)]^{2+}$.

The addition of more than 1 equiv of *t*BuOK gives rise to an appearance of a new band at 870 nm, accompanied with decrease in the absorption band at 576 nm due to $[Ru^{II}Q(OH^-)]^+$ (Figure 1). The characteristic absorption band at 870 nm is close to the MLCT bands of the Ru^{II}-semiquinone complexes, such as $[Ru^{II}(trpy)(35tBu_2SQ)(AcO^-)]$ (876 nm, $\varepsilon = 18600\,M^{-1}\,cm^{-1}$).[8] Two isosbestic points are observed at 720 and 657 nm in these two-step spectral changes. The addition of the same amount of $HClO_4$ as an acid to the solution fully recovered the 600 nm band.

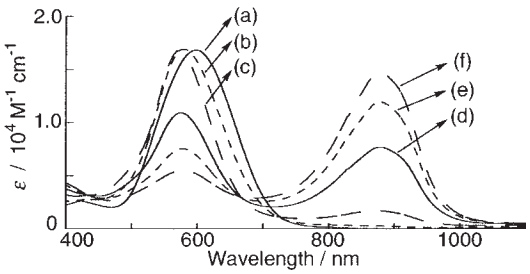

Figure 1. UV-vis spectra observed upon the addition of *t*BuOK ((a) 0 equiv; (b) 0.5 equiv; (c) 1.0 equiv; (d) 1.5 equiv; (e) 2.0 equiv; (f) 3.0 equiv) into a CH_2Cl_2 solution of **1** at 298 K.

The cyclic voltammograms of **1** in the presence of various amounts of *t*BuOK are shown in Figure 2. The CV of **1** exhibits two reversible redox waves at $E_{1/2a} = 0.31$ V and $E_{1/2b} = -0.47$ V (vs SCE). The reversible waves of $E_{1/2a}$ and $E_{1/2b}$ correspond to the $[Ru^{II}Q(OH_2)]^{2+}/[Ru^{II}SQ(OH_2)]^+$ redox couple and the $[Ru^{II}SQ(OH_2)]^+/[Ru^{II}Cat(OH_2)]$ one, respectively. The addition of 1 equiv of *t*BuOK into the solution of **1** results in appearances of new two redox waves at $E'_{1/2a} = 0.07$ V and $E'_{1/2b} = -0.57$ V (Figure 2B), which can be assigned to the $[Ru^{II}Q(OH^-)]^+/$

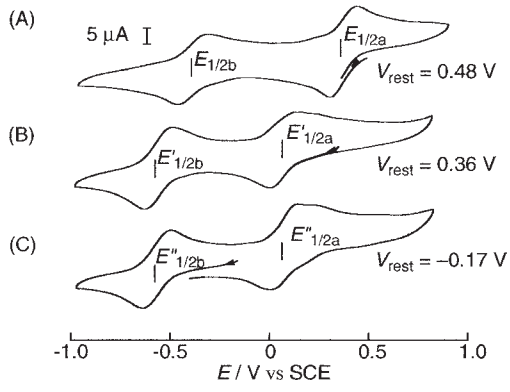

Figure 2. Cyclic voltammograms observed upon the addition of *t*BuOK ((A) 0 equiv, $V_{rest} = 0.48$ V; (B) 1.0 equiv, $V_{rest} = 0.36$ V; (C) 3.0 equiv, $V_{rest} = -0.17$ V) into CH_2Cl_2 solution of **1** (1.0 mM) containing 0.1 M TBAP; working electrode: glassy-carbon, counter electrode: Pt wire, reference electrode: Ag/Ag^+, scan rate: 100 mV s^{-1}. All CVs were started from V_{rest}.

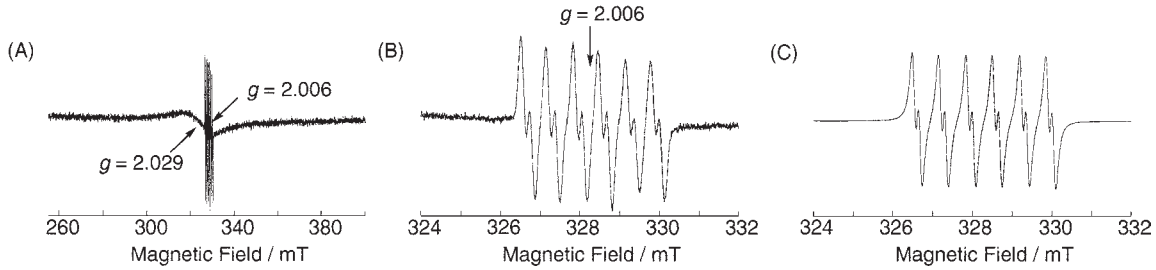

Figure 3. ESR spectra obtained upon the addition of 3.0 equiv of *t*BuOK and DMPO to a CH_2Cl_2 solution of **1** (2.0 mM) at 193 K ((A) and (B)). Shown in (C) is computer simulation of $[Ru^{II}(trpy)(3,5t\text{Bu}_2\text{SQ})(O)(DMPO)]$ ($g = 2.006$, $a_N{}^{\alpha} = 1.32$, $a_H{}^{\beta} = 0.63$ and $a_H{}^{\gamma} = 0.20$ mT). Microwave power is 1 mW and modulation amplitude is 0.14 mT.

$[Ru^{II}SQ(OH^-)]$ couple and the $[Ru^{II}SQ(OH^-)]/[Ru^{II}Cat(OH^-)]^-$ one based on the results of UV-vis spectral measurements.

The redox waves at 0.07 and −0.57 V do not change upon the addition of more than 1 equiv of *t*BuOK to the solution of $[Ru^{II}Q(OH^-)]^+$, on the other hand, the rest potential (V_{rest}) is dramatically negative-shifted to −0.17 V passing through the $[Ru^{II}Q(OH^-)]^+/[Ru^{II}SQ(OH^-)]$ redox couple (0.07 V) (Figure 2C). This result indicates that the quinone ligand is reduced to the semiquinone coupled with the deprotonation of the hydroxo ligand, which is consistent with the appearance of the characteristic MLCT band of Ru^{II} to semiquinone at 870 nm. Such characteristic behaviour is explained by the view that the first deprotonation of $[Ru^{II}Q(OH_2)]^{2+}$ just converts the aqua ligand (OH_2) to the hydroxo one (OH^-) [eq 1], and the deprotonation of the hydroxo ligand (OH^-) to an oxide ion ligand (O^{2-}) is accompanied with electron transfer from O^{2-} to quinone yielding the oxyl radical ligand ($O^{\bullet -}$) as [eq 2].

$$[Ru^{II}Q(OH_2)]^{2+} + t\text{BuOK} \rightleftharpoons [Ru^{II}Q(OH^-)]^+ + t\text{BuOH} \quad \text{(eq 1)}$$

$$[Ru^{II}Q(OH^-)]^+ + t\text{BuOK} \rightleftharpoons [Ru^{II}Q(O^{2-})] \updownarrow [Ru^{II}SQ(O^{\bullet -})] + t\text{BuOH} \quad \text{(eq 2)}$$

To confirm the Ru^{II}-semiquinone oxyl radical complex, $[Ru^{II}(trpy)(3,5t\text{Bu}_2\text{SQ})(O^{\bullet -})]$ generated in the deprotonation of aqua ligand, the ESR spin trapping technique by using of 5,5-dimethyl-1-pyrroline *N*-oxide (DMPO) is applied for detection and identification of the ruthenium oxyl radical complex.

The ESR spectrum obtained upon the addition of a 3 equiv of *t*BuOK and DMPO to a CH_2Cl_2 solution of **1** at 193 K is shown in Figure 3A and B. The ESR spectrum in Figure 3A shows an isotropic broad signal without hyperfine structure ($g = 2.029$, $\Delta H_{msl} = 7.3$ mT) together with 12-line sharp signal centred at $g = 2.006$ (Figure 3B). The pattern of ESR spectrum was not perturbed by a change of modulation amplitude within 0.14 mT. The hyperfine coupling constants values of the characteristic 12-line sharp signal ($g = 2.006$, $a_N{}^{\alpha} = 1.32$, $a_H{}^{\beta} = 0.63$ and $a_H{}^{\gamma} = 0.20$ mT) is determined by the computer simulation (Figure 3C). The ESR signal centred at $g = 2.029$ is very close to those of the Ru^{II}-semiquinone complex, $[Ru^{II}(trpy)(3,5t\text{Bu}_2\text{SQ})AcO^-]$[9] ($g = 2.030$, $\Delta H_{msl} = 8.0$ mT), thus, the isotropic broad signal ($g = 2.029$) can be assigned to the Ru^{II}-SQ moiety. As expected from the results of UV and CV, the signal intensity resulted from the Ru^{II}-SQ moiety linearly increased with increasing amounts of *t*BuOK, when more than 1 eq of *t*BuOK was added to the solution. The other ESR signal centred at $g = 2.006$ can be assigned to the DMPO spin adduct, $[Ru^{II}(trpy)(3,5t\text{Bu}_2\text{SQ})(O)(DMPO)]$[10] as shown in Scheme 1.

Formation of the DMPO spin adduct is further confirmed by

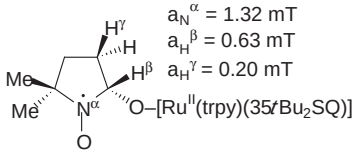

Scheme 1.

ESI mass spectrum which exhibited a signal at m/z 684. The observed mass and isotope patterns corresponded to $[Ru^{II}(trpy)(3,5t\text{Bu}_2\text{SQ})(^{16}O)(DMPO)]^+$. The labeling experiment using $H_2{}^{18}O$ showed an expected signal at m/z 686 correspond to $[Ru^{II}(trpy)(3,5t\text{Bu}_2\text{SQ})(^{18}O)(DMPO)]^+$, suggesting that an oxyl radical ligand was generated by the deprotonation of an aqua ligand.

In conclusion, oxyl radical is generated by taking advantage of the acid-base equilibrium of the aqua ligand coupled with the reduction of the quinone ligand. The ruthenium oxyl radical complex thus formed has been successfully characterized by using spin trapping technique.

We are grateful to Prof. Shunichi Fukuzumi, Department of Material and Life Science, Graduate School of Engineering, Osaka University, for the measurements of ESR spectra. This work was partially supported by a Grant-in-Aid for Scientific Research Priority Area (No. 12440190) from Ministry of Education, Science, Sports and Culture, Japan.

References and Notes

1 C. G. Pierpont and R. M. Buchanan, *Coord. Chem. Rev.*, **38**, 45 (1981).
2 C. G. Pierpont and C. W. Lange, *Prog. Inorg. Chem.*, **41**, 331 (1994).
3 A. Y. Girgis, Y. S. Sohn, and A. L. Balch, *Inorg. Chem.*, **14**, 2327 (1975); D. J. Gordon and R. F. Fenske, *Inorg. Chem.*, **21**, 2907 (1982).
4 S. Bhattacharya, S. R. Boone, G. A. Fox, and C. G. Pierpont, *J. Am. Chem. Soc.*, **112**, 1088 (1990); M. Haga, K. Isobe, S. R. Boone, and C. G. Pierpont, *Inorg. Chem.*, **29**, 3795 (1990).
5 S. R. Boone and C. G. Pierpont, *Inorg. Chem.*, **26**, 1769 (1987); A. P. B. Lever, P. R. Auburn, E. S. Dodsworth, M. Haga, W. Lei, M. Melnik, and W. A. Nevin, *J. Am. Chem. Soc.*, **110**, 8076 (1988); H. Masui, A. B. P. Lever, and P. R. Auburn, *Inorg. Chem.*, **30**, 2402 (1991); P. R. Auburn, E. S. Dodsworth, M. Haga, W. Liu, W. A. Nevin, and A. P. B. Lever, *Inorg. Chem.*, **30**, 3502 (1991); S. Bhattacharya and C. G. Pierpont, *Inorg. Chem.*, **33**, 6038 (1994).
6 B. A. Moyer and T. J. Meyer, *Inorg. Chem.*, **20**, 436 (1981); K. J. Takeuchi, M. S. Thompson, D. W. Pipes, and T. J. Meyer, *Inorg. Chem.*, **23**, 1845 (1984).
7 K. Tsuge and K. Tanaka, *Chem. Lett.*, **1998**, 1069; K. Tsuge, M. Kurihara, and K. Tanaka, *Bull. Chem. Soc. Jpn.*, **73**, 607 (2000).
8 M. Kurihara, S. Daniele, K. Tsuge, H. Sugimoto, and K. Tanaka, *Bull. Chem. Soc. Jpn.*, **71**, 867 (1998).
9 The characteristic 12-line sharp signal centred at $g = 2.006$ depicted in Figure 3B can not be observed in the addition of DMPO into a CH_2Cl_2 solution of the $[Ru^{II}(trpy)(3,5t\text{Bu}_2\text{SQ})AcO^-]$.
10 The signal of the DMPO spin adduct increased linearly with an increase in the DMPO concentration.